International Journal of Automotive Technology, Vol. 8, No. 6, pp. 731–744 (2007)

1229-9138/2007/037-08

DYNAMIC ANALYSIS AND DESIGN CALCULATION METHODS FOR POWERTRAIN MOUNTING SYSTEMS

W.-B. SHANGGUAN[1)*] and Y. ZHAO[2)]

[1)]College of Automotive Engineering, South China University of Technology, Guangzhou 510641, China
[2)]National CIMS Engineering Research Center, Tsinghua University, Beijing 100084, China

(Received 23 February 2007; Revised 19 October 2007)

ABSTRACT–A method for dynamic analysis and design calculation of a Powertrain Mounting System (PMS) including Hydraulic Engine Mounts (HEM) is developed with the aim of controlling powertrain motion and reducing low-frequency vibration in pitch and bounce modes. Here the pitch mode of the powertrain is defined as the mode rotating around the crankshaft of an engine for a transversely mounted powertrain. The powertrain is modeled as a rigid body connected to rigid ground by rubber mounts and/or HEMs. A mount is simplified as a three-dimensional spring with damping elements in its Local Coordinate System (LCS). The relation between force and displacement of each mount in its LCS is usually nonlinear and is simplified as piecewise linear in five ranges in this paper. An equation for estimating displacements of the powertrain center of gravity (C.G.) under static or quasi-static load is developed using Newton's second law, and an iterative algorithm is presented to calculate the displacements. Also an equation for analyzing the dynamic response of the powertrain under ground and engine shake excitations is derived using Newton's second law. Formulae for calculating reaction forces and displacements at each mount are presented. A generic PMS with four rubber mounts or two rubber mounts and two HEMs are used to validate the dynamic analysis and design calculation methods. Calculated displacements of the powertrain C.G. under static or quasi-static loads show that a powertrain motion can meet the displacement limits by properly selecting the stiffness and coordinates of the tuning points of each mount in its LCS using the calculation methods developed in this paper. Simulation results of the dynamic responses of a powertrain C.G. and the reaction forces at mounts demonstrate that resonance peaks can be reduced effectively with HEMs designed on the basis of the proposed methods.

KEY WORDS : Automotive powertrain mounting systems, Hydraulic engine mounts, Motion and vibration control of a powertrain, Analysis and calculation methods

NOMENCLATURE

K_c^* : complex stiffness of a mount
K' : storage stiffness of a mount
K'' : loss stiffness o f a mount
K_d : dynamic stiffness of a mount
ϕ : loss angle of a mount
C : damping coefficient of a mount
GCS : global coordinate system
LCS : local coordinate system of a mount
k_{ui}, k_{vi}, k_{wi} : static stiffness of the th mount in its LCS
x_i, y_i, z_i : location of the th mount in GCS.
k_u',k_v',k_w' : storage stiffness of a mount in its LCS
k_u'',k_v'',k_w'' : loss stiffness of a mount in its LCS
I_{XX}, I_{YY}, I_{ZZ}, I_{XY}, I_{YZ}, I_{ZX} : inertia properties of the powertrain in GCS

*Corresponding author. e-mail: shangguanwb99@tsinghua.org.cn

1. INTRODUCTION

A powertrain (an engine and a transmission) mounting system (PMS) generally consists of a powertrain (engine and gearbox) and several mounts connected to a base structure (Yu *et al.*, 2001). A mount used in PMS is usually a rubber mount (rubber boned to metal), or a hydraulic engine mount (HEM). The force versus displacement relation (F-D relation for short) of a rubber mount or an HEM is determined by its rubber components. The dynamic stiffness and loss angles of the two kinds of mounts under low-frequency and large-amplitude excitations are quite different (Yu *et al.*, 2001). One advantage of an HEM is that it can provide large damping around a frequency value (Shangguan and Lu, 2004). Motion control and vibration isolation of a powertrain are very common and important engineering design problems in automobiles and ships (Tao *et al.*, 2000). The challenge in designing a PMS is to select the appropriate

static and dynamic properties of the mounts and to install them properly to control powertrain motion, and to minimize the forces transmitted to the base structures, such as mount brackets and the car body. Unlike normal application inbuilding, a PMS in an automobile or ship engine can react to the strong quasi-static forces caused by cornering loads, impacts from road unevenness, wave slats, etc. (Tao *et al.*, 2000). Thus, a large static stiffness of mounts must be designed to keep the powertrain within the limits if the F-D relation of a mount in three directions of its local coordinate system (LCS) is linear. This will increase the forces transmitted to the structure. Thus, relation between the force and the displacement of a mount in its LCS is usually thought to be nonlinear and is simplified as piecewise linear.

In recent years, four-cylinder engines and transversely mounted powertrains, which worsen the influences of the powertrain vibration on the car body, have been widely used for cars. In controlling low-frequency vibrations of a powertrain, two kinds of excitations need to be considered. One is from the ground excitation, and another is due to the output torque changes in the engine. These two kinds of excitations are low-frequency and large-amplitude excitations and tend to excite larger vibrations of a powertrain. To control the vibration, the engine mount must be stiff and highly damped under the two kinds of excitations. However, when comparing dynamic performances of an HEM with its rubber mount, that the dynamic stiffness and damping of a rubber mount are nearly invariant with excitation amplitude and frequency over a range of 1 to 250 Hz (Shangguan and Lu, 2004). Consequently, at present, manufacturers have increasingly used an HEM in a PMS, which can provide large damping around a frequency under low-frequency and large-amplitude excitations. An HEM is selected mainly to control vibrations of a powertrain in pitch or bounce modes. Here, the pitch mode of the powertrain is defined as a mode rotating around the crankshaft of the engine for a transversely mounted powertrain.

There is a substantial body of literature dealing with the dynamic analysis and design calculation methods for a PMS (Bernard and Starkey, 2003; Brach, 1997; Cho, 2000; Geck and Patton, 1984; Johson and Subhedar, 1979; Qatu *et al.*, 2002; Shangguan and Lu, 2004; Swanson *et al.*, 1993; Suh *et al.*, 2003; Snyman *et al.*, 1995; Tao *et al.*, 2000 Vietor *et al.*, 1997; Yu *et al.*, 2001; Zavala *et al.*, 2000). In modeling a PMS, the powertrain is usually regarded as a rigid body and is supported by three or four mounts fixed to a rigid floor (Johson and Subhedar, 1979; Cho, 2000; Suh *et al.*, 2003). Most papers focus on selecting the stiffness, location and orientation of individual mounts by decoupling the pitch mode of a powertrain and locating the six frequencies of a powertrain rigid mode in the prescribed ranges (Johson, Subhedar, 1979; Cho, 2000), or by minimizing the forces transmitted to the structure (Suh *et al.*, 2003). In calculating displacements of a powertrain'scenter of gravity (C.G.) under static or quasi-static loads, most studies are conducted based on the assumption that the F-D relation of a mount in its LCS is linear (Brach, 1997; Swanson *et al.*, 1993). To the best of our knowledge, there is no method forestimating displacements of the powertrain C.G. when the F-D relation of a mount in its LCS is regarded as nonlinear and can be simplified as piecewise linear.

In analyzing low-frequency vibrations of a powertrain under dynamic force and torque excitations, most studies have regarded the mounts in a PMS as rubber mounts (Tao *et al.*, 2000 Swanson *et al.*, 1993). An analysis and design method was developed by Ishihama *et al.* to control powertrain vibrations in pitch and bounce modes during low-frequency vibrations (Ishihama *et al.*, 1995). They used a simple model with two degrees of freedom (DOF) to simulate the vibration characteristics of a PMS. Two HEMs or one HEM plus one rubber mount were used in the model to demonstrate the effectiveness of using HEMsfor controlling low-frequency vibrations of the powertrain in the pitch and bounce modes. However, the 2 DOF model seems too simple to simulate the performance of a generic PMS since the powertrain can move in six directions (three translation and three angle displacements) and the movements are possibly coupled. Therefore the chief objectives of this paper are to develop an analysis and design method for estimating the displacements of a powertrain C.G. when the F-D relation of a mount in its LCS is nonlinear and can be simplified as piecewise linear. Furthermore, the study aims to devise a design calculation method for a PMS using HEMs to control powertrain vibrations in bounce and pitch modes. A simplified 6 DOF model for a PMS is used in this paper. The model regards the powertrain as a rigid body that can move in six directions. The powertrain is supported by four mounts (four rubber mounts or two rubber mounts and two HEMs) fixed to a rigid structure.

2. POWERTRAIN MOUNTING SYSTEM EQUATIONS

2.1. Modeling of a PMS

The configuration of a PMS is shown in Figure 1(a). As the figure shows, a PMS consists of a powertrain and three or four mounts. The mounts used in a PMS are usually rubber mounts and /or HEMs. One end of a mount connects to the powertrain and another end connects to the car body or subframe. Figure 1(b) shows a simplified 6 DOF model. In modeling a PMS, the powertrain is regarded as a rigid body supported by three or four mounts, and can move in six directions. A mount

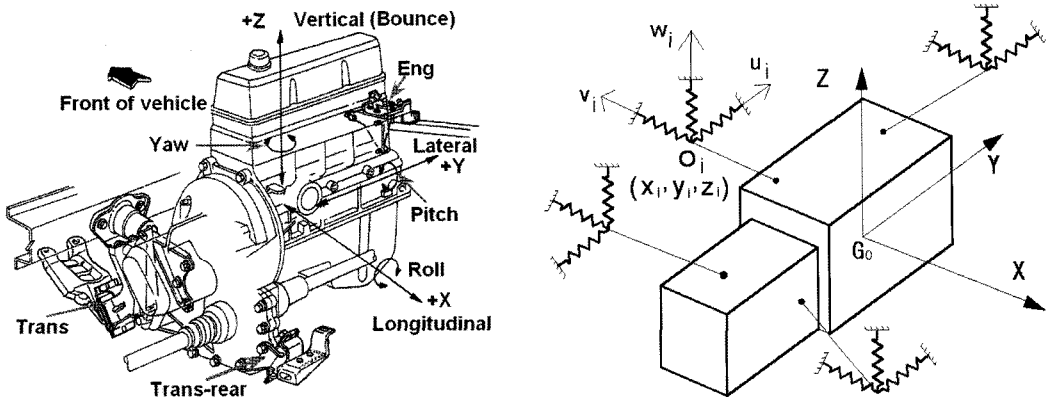

(a) Configuration (b) The simplified model

Figure 1. The configuration and the simplified 6 DOF model of a PMS.

is simplified as spring and damping elements in three orthogonal directions (Tao *et al.*, 2000; Qatu *et al.*, 2002; Swanson *et al.*, 1993; Snyman *et al.*, 1995). The end where the mountsconnects to the car body or subframe is assumed to be fixed to a rigid structure as shown in Figure 1(b). Although some researchers established a complex PMS model including the flexibility of base structures (Demic, 1990), the conclusion obtained by Sirafi and Qatu (Sirafi and Qatu, 2003) suggested that the 6 DOF model including rigid base structures is good enough to analyze dynamic performances of PMS in the preliminary design phase.

A right-hand Global Coordinate System (GCS), G_0-XYZ, which has its origin at the *C.G.* of the powertrain in its static equilibrium, is built to describe the movements of the powertrain. Here, the static equilibrium is defined as the position of the powertrain at rest under its dead weight. The three orthogonal coordinate axes are set with X- and Y- axes parallel to the horizontal plane, Z- axis normal to the plane, and the positive direction of X- axis points to the rear of a vehicle. A LCS, Q_i-$u_iv_ix_i$, is built for each mount, where the origin is at the connecting point of the mount and the powertrain, and the three coordinate axes are expressed by u_i, v_i and w_i (i=1,2,... n, where n is the number of mounts), respectively, which are perpendicular to one another.

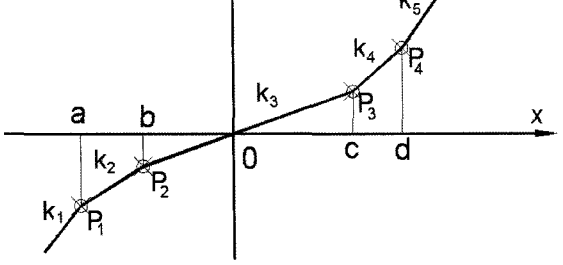

Figure 2. F-D relation of a mount in one direction of its LCS.

The static performances (F-D relation) of either a rubber mount or an HEM are determined by its rubber components (Shangguan and Lu, 2004). The relation between force and displacement for a mount in one direction of its LCS is usually nonlinear (Brach, 1997) and can be simplified as piecewise linear. Figure 2 shows the piecewise linearity at five ranges. If it is simplified with three ranges, the stiffness in ranges two (k_2) and four (k_4) equal the stiffness in the linear range (k_3). In Figure 2, points P_1, P_2, P_3 and P_4 are tuning points, in which P_1 and P_4 are defined as hard stop points and P_2 and P_3 are as the soft ones. The values a, b, c and d are x-coordinates of the hard or the soft points. The parameters k_1, k_2, k_3, k_4 and k_5 are stiffness values in corresponding ranges.

Complex stiffness (K_c^*) is used to characterize the dynamic behavior of a mount in u_i-, v_i- and w_i- directions of its LCS and is defined by (Shangguan and Lu, 2004).

$$K_c^*=K'+jK'' \tag{1}$$

where K' and K'' are storage stiffness and loss stiffness, respectively. The dynamic stiffness, K_d, loss angle, ϕ, and damping coefficient, C, of a mount are calculated from (Shangguan and Lu, 2004).

$$K_d=\sqrt{K'^2+K''^2},\ \phi=\tan^{-1}(K''/K'),\ C=\frac{K_d\sin\phi}{2\pi f} \tag{2}$$

where f is the excitation frequency.

Dynamic performances of a rubber mount and an HEM under low-frequency and large-amplitude excitations are quite different, and the performance comparisons of an HEM and its rubber spring can be found in the paper (Shangguan and Lu, 2004). One advantage of an HEM is that it can provide peak damping around a frequ-

Table 1. Values for k and Δ

range	k	Δ
Range 1 (-∞, a]	k_1	$-k_1a+k_2(a-b)+k_3b$
Range 2 (a, b]	k_2	$-k_2b+k_3b$
Range 3 (b, c]	k_3	0
Range 4 (c, d]	k_4	k_3c-k_4c
Range 5 (d, +∞)	k_5	$k_3c-k_4c+k_4d-k_5d$

ency value, which can decrease the vibration amplitude of a powertrain very quickly.

2.2. Equations for Calculating Displacements of the Powertrain C.G. under Static Loads

For calculating the displacement of a powertrain C.G. under static or quasi-static forces, only static properties of a mount are needed. The static stiffness of the mount i (i=1,2,.....n, where n is the number of mounts) in u_i-, v_i- and w_i- directions of its LCS are represented by k_{ui}, k_{vi} and k_{wi}, respectively.

The F-D relation shown in Figure 2 is described mathematically by Equation (3)

$$F=kx+\Delta \tag{3}$$

where k and Δ are stiffness and correction term, and their values can be obtained with formulae in Table 1 when displacement, x, is determined.

The F-D relation of the mount i in its LCS is written as

$$\mathbf{f}_i=\mathbf{k}_i\bar{\mathbf{U}}_i+\Delta_i \tag{4}$$

where $\mathbf{k}_i=diag\,(k_{ui}, k_{vi}, k_{wi})$ is the static stiffness matrix of the mount i in its LCS; $\bar{\mathbf{U}}_i$ and $\mathbf{f}_i$ are the displacement and force vectors of the mount i in its LCS; Δ_i is the correction vector and is expressed as $\Delta_i=(\Delta_{ui}, \Delta_{vi}, \Delta_{wi})^T$, where Δ_{ui}, Δ_{vi} and Δ_{wi} are correction terms of the mount i in u_i-, v_i- and w_i- directions. The components in $\mathbf{k}_i$ and Δ_i can be obtained with the formulae in Table 1 according to the components in $\bar{\mathbf{U}}_i$.

To express the F-D relation of a mount in GCS, one gets

$$\mathbf{F}_i=\mathbf{K}_i^*\mathbf{U}_i+\mathbf{A}_i\Delta_i \tag{5}$$

where

$$\mathbf{K}_i^*=\mathbf{A}_i\mathbf{k}_i\mathbf{A}_i^T \tag{6}$$

is the stiffness matrix of the mount i in GCS; $\mathbf{U}_i$ and $\mathbf{F}_i$ are the displacement and force vectors of the mount i in GCS, respectively; $\mathbf{A}_i$ the transformation matrix from LCS of the mount i to GCS. The transformation matrix can be easily formed from the orientations of the mount with respect to GCS (Haug, 1989), which can be defined using Euler angles or direction cosines, etc.

The transformation of powertrain C.G., $\mathbf{X}$, to the translation displacement at the mounting point in GCS can be written as (Haug, 1989)

$$\mathbf{U}_i=[\mathbf{I}\ -\tilde{\mathbf{r}}_i]\mathbf{X} \tag{7}$$

where $\mathbf{I}$ is the (3×3) unity matrix; $\tilde{\mathbf{r}}_i$ is the (3×3) skew-symmetric matrix of the mount i position vector, $\mathbf{r}_i$, with respect to powertrain C.G.; that is, given

$$\mathbf{r}_i=x_i\vec{i}+y_i\vec{j}+z_i\vec{k} \tag{8}$$

the skew-symmetric matrix, $\tilde{\mathbf{r}}_i$, is expressed as (Haug, 1989)

$$\tilde{\mathbf{r}}_i=\begin{bmatrix}0 & -z_i & y_i\\ z_i & 0 & -x_i\\ -y_i & x_i & 0\end{bmatrix} \tag{9}$$

where x_i, y_i and z_i are locations of the mount i in GCS. Substituting Equation (7) into Equation (5), one gets

$$\mathbf{F}_i=[\mathbf{K}_i^*\ -\mathbf{K}_i^*\tilde{\mathbf{r}}_i]\mathbf{X}+\mathbf{A}_i\Delta_i \tag{10}$$

In terms of a powertrain displacement, the transmitted force vector to the powertrain from the force $\mathbf{F}_i$ is

$$\mathbf{RFM}_i=-\mathbf{F}_i=-[\mathbf{K}_i^*\ -\mathbf{K}_i^*\tilde{\mathbf{r}}_i]\mathbf{X}-\mathbf{A}_i\Delta_i \tag{11}$$

The moment vector, $\mathbf{RMM}_i$, which results from the force vector of mount i, $\mathbf{RFM}_i$, on the powertrain C.G. is

$$\begin{aligned}\mathbf{RMM}_i&=\mathbf{r}_i\times\mathbf{RFM}_i=\tilde{\mathbf{r}}_i\mathbf{RFM}_i\\&=[\tilde{\mathbf{r}}_i^T\mathbf{K}_i^*\ -\tilde{\mathbf{r}}_i^T\mathbf{K}_i^*\tilde{\mathbf{r}}_i]\mathbf{X}-\tilde{\mathbf{r}}_i\mathbf{A}_i\Delta_i\end{aligned} \tag{12}$$

Combining Equations (11) and (12) yields

$$\begin{aligned}\mathbf{EFM}_i&=\{\mathbf{RFM}_i,\ \mathbf{RMM}_i\}^T\\&=\begin{bmatrix}-\mathbf{K}_i^* & \mathbf{K}_i^*\tilde{\mathbf{r}}_i\\ \tilde{\mathbf{r}}_i^T\mathbf{K}_i^* & -\tilde{\mathbf{r}}_i^T\mathbf{K}_i^*\tilde{\mathbf{r}}_i\end{bmatrix}\mathbf{X}-\begin{Bmatrix}\mathbf{A}_i\Delta_i\\ \tilde{\mathbf{r}}_i^T\mathbf{A}_i\Delta_i\end{Bmatrix}\end{aligned} \tag{13}$$

where $\mathbf{EFM}_i$ is defined as a generalized load vector resulting from the mount i which encompasses both forces and moments of the powertrain C.G. in all six DOFs.

By summing all of the forces from a total of n mounts, the total load vector on the powertrain C.G. can be expressed as

$$\mathbf{EFM}=\sum_{i=1}^{n}\mathbf{EFM}_i=\begin{bmatrix}-\sum_{i=1}^{n}\mathbf{K}_i^* & \sum_{i=1}^{n}\mathbf{K}_i^*.\tilde{\mathbf{r}}_i\\ \sum_{i=1}^{n}\tilde{\mathbf{r}}_i^T\mathbf{K}_i^* & -\sum_{i=1}^{n}\tilde{\mathbf{r}}_i^T\mathbf{K}_i^*.\tilde{\mathbf{r}}_i\end{bmatrix}\mathbf{X}-\begin{Bmatrix}\sum_{i=1}^{n}\mathbf{A}_i\Delta_i\\ \sum_{i=1}^{n}\tilde{\mathbf{r}}_i\mathbf{A}_i\Delta_i\end{Bmatrix} \tag{14}$$

With all the components of reactive forces derived in terms of the displacements of powertrain C.G., the equation for analyzing the powertrain motion under static or quasi-static loads can be obtained using Newton's second law

$$\mathbf{K}\,\mathbf{X}=\mathbf{EF}-\mathbf{Delta} \tag{15}$$

where

$$\mathbf{K}=\begin{bmatrix} -\sum_{i=1}^{n}\mathbf{K}_i^* & -\sum_{i=1}^{n}\mathbf{K}_i^*.\tilde{\mathbf{r}}_i \\ \sum_{i=1}^{n}\tilde{\mathbf{r}}_i^T\mathbf{K}_i^* & \sum_{i=1}^{n}\tilde{\mathbf{r}}_i^T\mathbf{K}_i^*.\tilde{\mathbf{r}}_i \end{bmatrix} \tag{16}$$

$$\mathbf{Delta}=\begin{Bmatrix} \sum_{i=1}^{n}\mathbf{A}_i\Delta_i \\ \sum_{i=1}^{n}\tilde{\mathbf{r}}_i\cdot\mathbf{A}_i\Delta_i \end{Bmatrix} \tag{17}$$

The vector **EF** in Equation (15) represents the external static or quasi-static force vector applied to the powertrain C.G..

2.3. Equations for Dynamic Response Analysis of a Powertrain

Based on Equation (1), the complex stiffness matrix of the mount i in its LCS, $\mathbf{k}_{id}^*$, can be written as

$$\mathbf{k}_{id}^*=\begin{bmatrix} k_u'+jk_u'' & & \\ & k_v'+jk_v'' & \\ & & k_w'+jk_w'' \end{bmatrix} \tag{18}$$

where k_u', k_v', and k_w' are the storage stiffness of the mount i in u_i-, v_i- and w_i- directions of its LCS, respectively; k_u'', k_v'' and k_w'' are losses stiffness of the mount i in u_i-, v_i- and w_i- directions of its LCS, respectively.

This complex stiffness matrix must be transformed from LCS of the mount to GCS through the following linear transformation:

$$\mathbf{K}_{id}^*=\mathbf{A}_i\mathbf{k}_{id}^*\mathbf{A}_i^T \tag{19}$$

where $\mathbf{A}_i$ is the transform matrix defined in Equation (6).

In deriving dynamic response equations of a powertrain, two kinds of excitations must be considered. One is from the ground in the three translation directions of GCS, but the excitation from the vertical direction is usually dominant. Another is due to the changes of the powertrain output torque. The two kinds of excitations tend to make the powertrain vibrate in bounce and pitch directions. Assuming the displacement excitation to mount i from the rigid structure in GCS is $\mathbf{U}_{ig}$, the displacement excitation to the mount in its LCS, $\bar{\mathbf{U}}_{igd}$, is then estimated by

$$\bar{\mathbf{U}}_{igd}=\mathbf{A}_i^T\mathbf{U}_{ig} \tag{20}$$

The force of mount i in GCS, $\mathbf{F}_{id}$, is then calculated by

$$\mathbf{F}_{id}=\mathbf{K}_{id}^*\mathbf{U}_i+\Delta_{id} \tag{21}$$

where Δ_{id} is a correction vector and is expressed as

$$\Delta_{id}=-\mathbf{K}_{id}^*\mathbf{U}_{ig} \tag{22}$$

By using the similar approaches in Section 2.2 and Newton's second law, the dynamic equations of a powertrainare obtained and written as

$$\mathbf{M}\mathbf{X}_d+\mathbf{K}_d\mathbf{X}_d=\mathbf{F}+\mathbf{F}_g \tag{23}$$

where

$$\mathbf{K}_d=\begin{bmatrix} \sum_{i=1}^{n}\mathbf{K}_{id}^* & -\sum_{i=1}^{n}\mathbf{K}_{id}^*.\tilde{\mathbf{r}}_i \\ -\sum_{i=1}^{n}\tilde{\mathbf{r}}_i^T\mathbf{K}_{id}^* & \sum_{i=1}^{n}\tilde{\mathbf{r}}_i^T\mathbf{K}_{id}^*.\tilde{\mathbf{r}}_i \end{bmatrix} \tag{24}$$

$$\mathbf{F}_g=\begin{Bmatrix} \sum_{i=1}^{n}\Delta_{id} \\ \hline \sum_{i=1}^{n}\tilde{\mathbf{r}}_i\sum_{i=1}^{n} \end{Bmatrix} \tag{25}$$

The complex stiffness matrix, $\mathbf{K}_d$, in Equation (24) is calculated based on complex stiffness matrix of the individual mount i, $\mathbf{K}_{id}^*$, and the location of mount i. The mass matrix **M** is a 6×6 constant matrix consisting of inertia properties of a powertrain (Swanson *et al.*, 1993); $\mathbf{X}_d=\{x, y, z, \theta_x, \theta_y, \theta_z\}^T$ is the dynamic displacement vector of the powertrain C.G.; **F** is a 6×1 vector of excitation force induced by the torque changes; $\mathbf{F}_g$ is a 6×1 excitation force vector induced by the displacement excitation from the rigid structure.

3. SOLUTIONS TO THE EQUATIONS

3.1. Iterative Algorithms for Solving Displacements of a Powertrain under Static or Quasi-static Loads

In obtaining displacements of a powertrain C.G. under static and quasi-static loads, the rigid structure is assumed to be fixed. Since the component values in stiffness, **K**, in Equation (16) depend on the magnitude of external forces, iterative algorithms must be used to determine the displacements of the powertrain C.G.. The steps are described as follows.

Step 1: Calculate displacements of each mount in its LCS under the powertrain weight load.

The displacements of each mount in its LCS should be in linear range and the **Delta** in Equation (15) should be zero under the powertrain weight. The displacements of powertrain C.G. are obtained by constituting Equation (15) and then solving the equation. The displacement vector of each mount in its LCS, $\bar{\mathbf{U}}_i$, is then calculated with Equations (15), (7) and (26).

$$\bar{\mathbf{U}}_i=\mathbf{A}_i^T\mathbf{U}_i \tag{26}$$

Step 2: Move the origin of the F-D relation curve in Figure 2 for each mount in its LCS to the point where the

displacement of a mount in its LCS is equal to that obtained in step 1.

Step 3: Apply external forces to powertrain C.G. in one loading condition and calculate the displacements of powertrain C.G. by solving Equation (15), assuming the displacements of each mounts in its LCS are in linear ranges.

Step 4: Get the displacements of each mount in its LCS using Equations (7) and (26).

Step 5: Check the displacements of each mount obtained in step 4 to see if they are in the linear range. If yes, output the actual displacements and then stop. The actual displacements of each mount in its LCS under the load result from a summation of the calculated displacement in step 4 and the displacement estimated in step 1; if no, record the ranges where the displacements are located, and then go to next the step.

Step 6: Constitute the new matrices of $\mathbf{k}_i$ and Δ_i in Equation (4) with the range data in step 5 and the formulae in Table 1, and then form the stiffness matrix, **K**, and correction vector, **Delta**, by using Equations (16) and (17), respectively.

Step 7: Find the displacements of powertrain C.G. by solving for newly formed Equation (15). Obtain the displacements of a mount in its LCS with Equations (15) and (26).

Step 8: Check the displacements of each mount in its LCS obtained in step 7 to see which ranges the displacements are located in and record them. If they are the same as that in step 5, output the calculated results and then stop, otherwise, go to step 6.

In some loads, the results may not converge after sufficient repeat calculations due to the inappropriate values for some stiffness and/or coordinates of the tuning points. So interruptions in the program should be designed.

The reaction forces at each mount can be determined by the formula (10) with the displacements of each mount. These reaction forces are important boundary conditions for the design of strength and fatigue life of mount brackets, and loading conditions for fatigue experiments of the mounts.

3.2. Solution to the Dynamic Equation of a Powertrain

Assuming the powertrain is fixed to a rigid structure, the natural frequencies and mode shapes of a powertrain are obtained from (Suh *et al.*, 2003; Demic, 1990)

$$|\mathbf{K} - \omega^2\mathbf{M}|=0 \tag{27a}$$

$$[\mathbf{K} - \omega_i^2\mathbf{M}]\varphi_i=0 \tag{27b}$$

where **M** is the (6×6) mass matrix containing inertia parameters of the powertrain (Swanson *et al.*, 1993); $\varphi=[\vec{\varphi}_1\ \vec{\varphi}_2\ \dots\ \vec{\varphi}_6]$ the (6×6) mode matrix, in which each column (6×1) represents translation and angle displacements of the six DOFs of the powertrain with respect to its C.G. in GCS; **K** is the (6×6) stiffness matrix and is a function of the dynamic stiffness, locations and orientations of the mounts (Tao *et al.*, 2000). The dynamic stiffness of a mount for analyzing the natural frequencies of the powertrain using Equation 27(a) equals the static stiffness (the K_3 in Figure 2) times a dynamic-to-static ratio of a mount, which is in the range of 1.1 to 1.6 depending on the Shore hardness of the rubber in the mount (Shangguan and Lu, 2004).

Solution of Equation (27) leads to a set of natural frequencies of the powertrain, $f_i(=\omega_i/2\pi, i=1, 2, \dots 6)$, and the corresponding mode vectors $\vec{\varphi}_i=(\varphi_{1i}, \varphi_{2i}, \dots, \varphi_{6i})^T$. When the powertrain vibrates at a natural frequency (f_i), the mode kinetic energy distribution (usually defined as the decoupling ratio) in the $n(n=1, 2\dots6)$ DOF of the powertrain and i-order mode, $E(n,i)$, is estimated from (Demic M, 1990)

$$E(n,i)=\frac{\frac{1}{2}\omega_i^2\varphi_{ni}\sum_{l=1}^{6}m_{nl}\varphi_{li}\quad\varphi_{ni}\sum_{l=1}^{6}m_{nl}\varphi_{li}}{\frac{1}{2}\omega_i^2\vec{\varphi}_i^T\mathbf{M}\vec{\varphi}_i}=\frac{}{\vec{\varphi}_i^T\mathbf{M}\vec{\varphi}_i} \tag{28}$$

where φ_{ni} is the nth element in the mode vector $\vec{\varphi}_i$, and m_{nl} is the element of the mass matrix, **M**, in n- row and l-column.

The response of the powertrain C.G. to the dynamic input can be calculated by solving Equation (23). In the frequency domain, the dynamic displacement vector of the powertrain C.G., $\mathbf{X}_d$, is expressed as

$$\mathbf{X}_d(f)=(-(2\pi f)^2\mathbf{M}+\mathbf{K}_d(f))^{-1}(\mathbf{F}(f)+\mathbf{F}_g(f)) \tag{29}$$

Equation (29), $\mathbf{F}(f)$ is assumed to be zero if only the excitation from a rigid structure is considered. If the excitations to the powertrain are only from torque changes due to the output power of changes in the engine, $\mathbf{F}_g(f)$ is set to zero.

The dynamic forces transmitted to mount i in GCS is then calculated by

$$\mathbf{F}_{id}=[\mathbf{K}_{id}^*\ -\mathbf{K}_{id}^*.\tilde{\mathbf{r}}_i]\mathbf{X}_d \tag{30}$$

4. APPLICATION EXAMPLE

4.1. Parameters of a Generic PMS

A generic PMS consisting of four mounts and a powertrain transversely mounted is shown in Figure 3. The Trans and Trans-rear mounts are rubber mounts. The powertrain weights 215 Kg, and its inertia properties are given in Table 2. The location and orientation of each mount is listed in Tables 3 and 4, respectively. Direction cosines are used to represent the orientation of the mounts in LCS with respect to GCS. The static stiffness and the coordinates of tuning points for each mount in three directions of its LCS are shown in Table 5. For

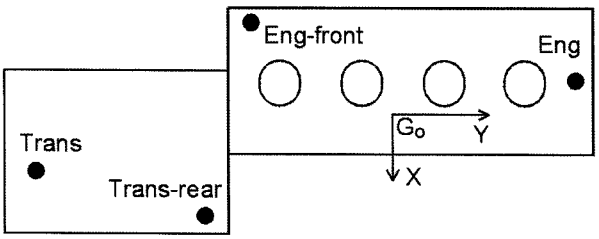

Figure 3. A PMS with four mounts.

Table 2. Inertia properties of a powertrain in GCS (Kg.m^2).

I_{XX}	I_{YY}	I_{ZZ}	I_{XY}	I_{YZ}	I_{ZX}
15.849	7.2663	12.5897	−0.7965	2.9916	0.0677

Table 3. Mount locations.

Mount	Coordinates in GCS (mm)		
	X	Y	Z
Eng	−42.5	506.6	181
Trans	57	−448.3	181
Eng-front	−267	−22	−146
Trans-Rear	315	−37	−209

Trans and Trans-rear mounts, the dynamic-to-static stiffness ratio is 1.2 and the loss angle is set to 6 degrees from the experimental data.

4.2. Static Displacement Results

Two loads (static or quasi-static force) along with the powertrain weight are considered to calculate the static deflection of a powertrain C.G.. The first load is a 'gee' force acting at the powertrain C.G. in vertical (Z) and right (Y) directions of GCS, and equal to 3.5 mg and 2 mg, respectively, where m is the powertrain mass and g is gravitational acceleration. The second load is a torque force of 6200 N.m around the Y- axis of GCS (pitch direction). The calculated static displacement of the powertrain C.G., and the displacements and the reaction forces at the four mounts are listed in Tables 6 to 9, respectively.

Displacements of powertrain C.G. under load 1 are shown in Table 6. It is seen that the displacement in the X-axis, the angles around X-, Y- and Z-axis can be nearly ignored. Since the powertrain translates only in the Y- and Z- directions under load 1, the posture of the

Table 4. Mount orientations (Degree).

Mount	LCS of a mount	GCS		
		X	Y	Z
Eng	u_i	0	90	90
	v_i	90	0	90
	w_i	90	90	0
Trans	u_i	0	90	90
	v_i	90	0	90
	w_i	90	90	0
Eng-front	u_i	34	90	56
	v_i	90	0	90
	w_i	124	90	34
Trans-rear	u_i	45	90	135
	v_i	90	0	90
	w_i	45	90	45

Table 5. Static stiffness under the preload of powertrain weight and x coordinate of the tuning points for each mount.

Mount	LCS of a mount	Stiffness for piecewise linear (N/mm)					x-coordinate of tuning points (mm)			
		k_1	k_2	k_3	k_4	k_5	p_1	p_2	p_3	p_4
Eng	u_i	2000	1100	150	1100	2000	−8	−5	5	8
	v_i	2000	550	140	550	2000	−8	−7	5	8
	w_i	840	340	160	640	600	−17	−13.5	2	5
Trans	u_i	1500	800	80	800	1500	−9.5	−5.5	5.5	9.5
	v_i	2000	1000	150	1000	2000	−8	−7	5	8
	w_i	1000	400	190	190	800	−17	−13.5	3	5
Eng-front	u_i	1200	650	160	650	1200	−19	−15	15	19
	v_i	2000	700	45	700	2000	−8	−7	7	8
	w_i	2250	1200	95	1200	2250	−13	−9.5	9.5	12
Trans-rear	u_i	1500	600	120	600	1500	−15	−12	12	15
	v_i	2000	500	40	500	2000	−8	−7	7	8
	w_i	3000	1305	75	1305	3000	−14	−10	10	14

Table 6. Displacements of the powertrain C.G. in GCS under load 1.

Translation displacement (mm)			Rotation angle (Deg)		
X	Y	Z	Roll (θ_X)	Pitch (θ_Y)	Yaw (θ_Z)
−0.2323	6.502	10.7852	0.0169	−0.0481	−0.0678

Table 7. Displacements and reaction forces of the four mounts under load 1.

Mount	Displacement in GCS (mm)			Reaction force in GCS (N)			Displacement in LCS (mm)		
	X	Y	Z	X	Y	Z			
Eng	0.2154	6.4989	4.7133	32.3	1524.4	2056.5	0.2154	6.4989	4.7133
Trans	−0.9149	6.3813	4.8404	−73.2	2131.3	919.7	−0.92	6.3813	4.8404
Eng-front	−0.059	6.861	10.1994	299.1	308.7	1174.5	5.6545	6.8609	8.4887
Trans-rear	−0.0115	6.1902	11.4272	−258.2	247.6	1114.4	−8.088	6.1902	8.0721

Table 8. Displacements of the powertrain C.G. in GCS under load 2.

Translation displacement (mm)			Rotate angle (Deg)		
X	Y	Z	Roll (θ_X)	Pitch (θ_Y)	Yaw (θ_Z)
0.9202	−0.5435	1.0261	−0.2979	2.5409	0.1532

Table 9. Displacements and reaction forces of the four mounts under load 2.

Mount	Displacement in GCS (mm)			Reaction force in GCS (N)			Displacement in LCS (mm)		
	X	Y	Z	X	Y	Z	u_i	v_i	w_i
Eng	7.5927	0.2838	−5.9084	3602.0	39.7	−945.3	7.5928	0.2838	−5.9084
Trans	10.1454	0.5495	−5.027	4608.1	82.4	−955.1	10.145	0.5495	−5.027
Eng-front	−5.4235	−2.0162	12.617	−3133.8	−90.7	5378.2	2.5591	−2.016	13.4927
Trans-rear	−8.1547	−0.7861	−12.384	−5076.3	−31.5	−5583.8	2.9901	−0.786	−14.5226

powertrain is almost the same as that of its static equilibrium.

The F-Drelations of Eng and Trans mounts in the three axial directions, and the reaction forces and the displacements acting on the two mounts under load 1 are shown in Figure 4. It is seen that the displacement of Eng and Trans mounts in v_i- and w_i- directions of its LCS are in the nonlinear range (range 4). However, the calculation results (comparing Table 7 with Table 5) show that the displacements of Eng-front and Trans-rear mounts in each of its LCS are only in the linear range (range 3). It is concluded that some of displacements of a mount in its LCS are located in the nonlinear section, while others are still in the linear section. The nonlinear section of Eng and Trans mounts in v_i- and w_i- directions of its LCS are used to control powertrain motion.

It is seen from Table 8 that the powertrain mainly rotates around the Y- axis of the GCS under load 2, which demonstrates that the posture of the powertrain under this load is a result of rotation of the powertrain in its static equilibrium.

The F-D relations of Eng, Trans and Trans-rear mounts in u_i- or w_i- direction, and the reaction forces and the displacements acting on the three mounts under load 2 are shown in Figure 5. It is evident that the displacements of Eng and Trans mounts in the u_i- axis are in the nonlinear range (range 4 and range 5 for Eng and Trans mounts, respectively), and the displacement of Trans-rear mount in w_i- axis is also in the nonlinear range (range 1).

The reaction forces at the four mounts listed in Tables 7 and 9 and the external loads are in equilibrium, which verifies the calculated results of the reaction forces. These reaction forces are important load conditions for strength design and fatigue experiments of mount brackets.

4.3. Dynamic Response of the Powertrain

The calculated natural frequencies and decoupling ratios of the powertrain are given in Table 10. It is seen that vibrations of the powertrain in bounce and pitch directions, in which the natural frequencies of the powertrain equal to 9.3 Hz and 11.6 Hz, respectively, are almost

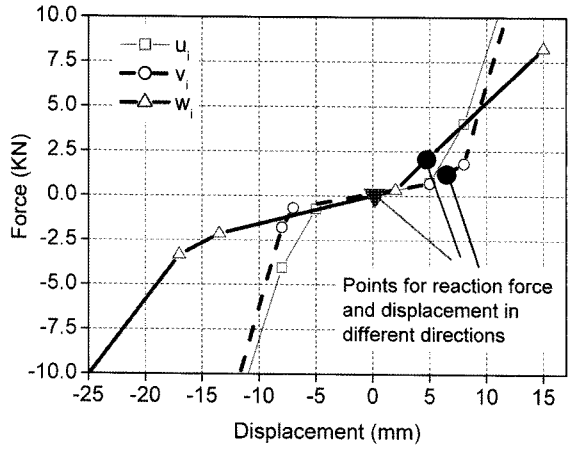

(a) Eng mount

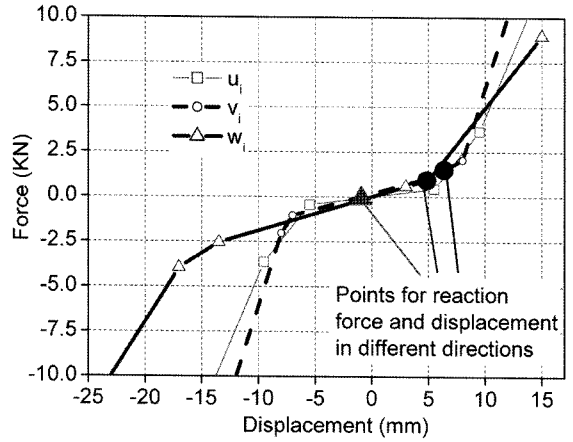

(b) Trans mount

Figure 4. The force versus the displacement relations of a mount in its LCS, and the reaction forces and displacements acting on the mount under load 1.

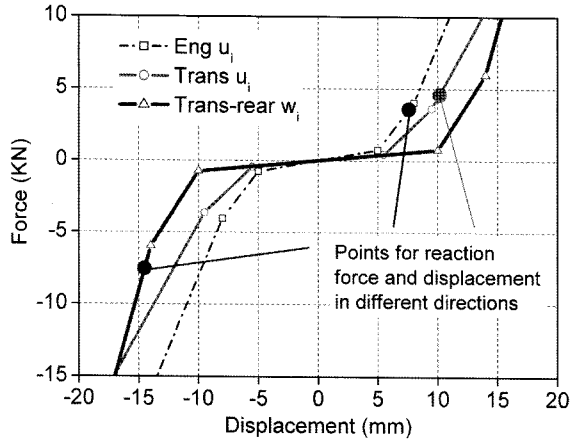

Figure 5. The force versus the displacement relations of the mounts in its LCS, and the reaction forces and displacements acting on the mounts under the load 2.

Table 10. Natural frequencies and decoupling ratios of a PMS in GCS.

Frequencies (Hz)		8.01	7.30	9.27	14.20	11.62	13.18
Decoupling ratios	X	**90.40**	0.04	0.55	0.01	6.74	2.27
	Y	0.07	**96.73**	0.11	2.09	0.50	0.52
	Z	0.51	0.06	**99.08**	0.29	0.06	0.00
	Roll	0.02	2.95	0.18	**85.92**	4.06	6.87
	Pitch	4.94	0.20	0.05	7.16	**86.99**	0.66
	Yaw	4.06	0.02	0.04	4.54	1.65	**89.68**

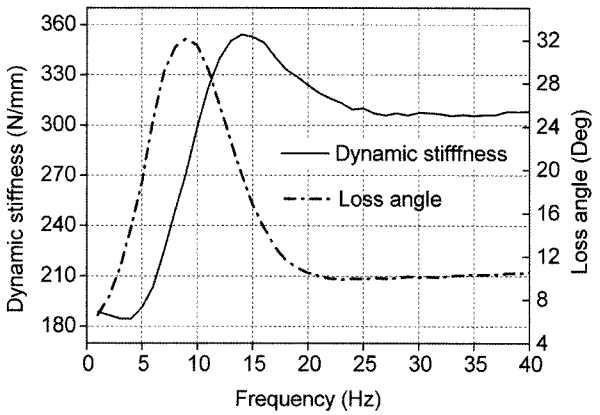

Figure 6. Dynamic stiffness and loss angle of the Eng mount.

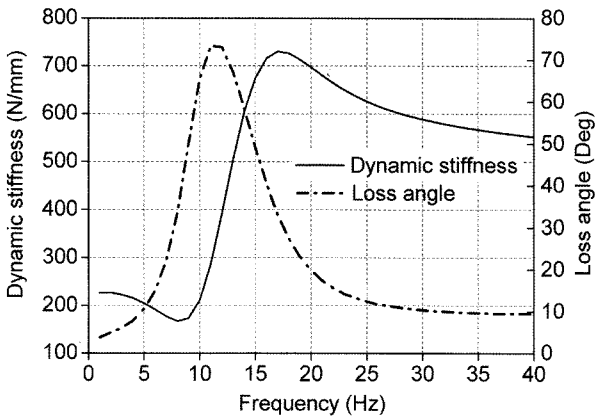

Figure 7. Dynamic stiffness and loss angle of the Eng-front mount.

decoupled from other modes since the decoupling ratios in the two directions are greater than 85%.

The excitations to a powertrain in an automotive PMS are mainly from bounce excitation (ground excitation) in the Z- direction and torque excitation in the pitch direction of GCS. To control vibration of the powertrain in bounce and pitch directions, one or two mounts in the

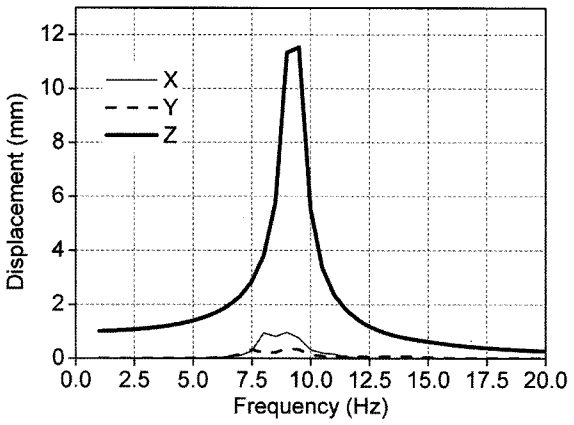

(a) Translation displacement

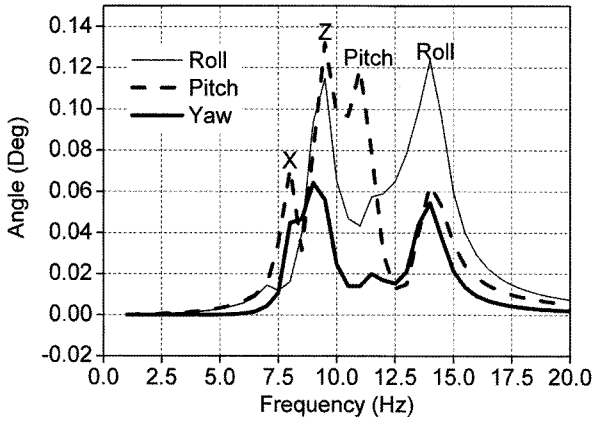

(b) Angle

Figure 8. The amplitude versus response of the powertrain C.G. for PMS I under ground excitation.

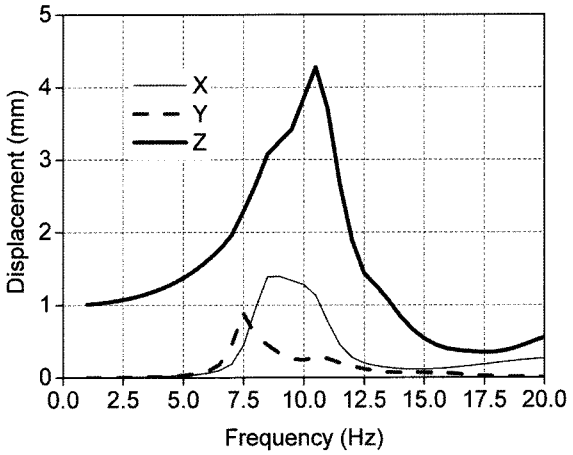

(a) Translation displacement

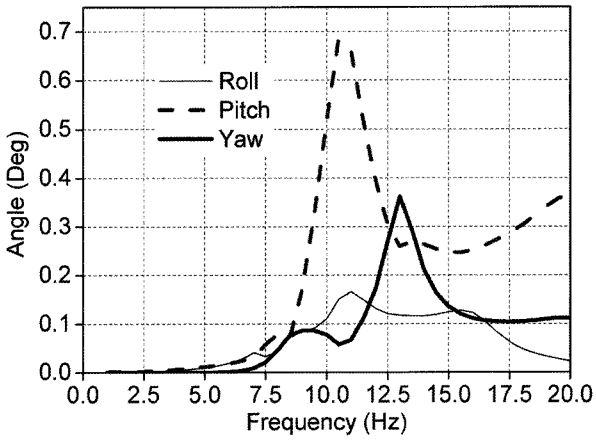

(b) Angle

Figure 9. The amplitude versus frequency response of the powertrain C.G. for PMS II under ground excitation.

PMS are usually of HEMs. If two HEMs are used in a PMS, the peak frequencies of loss angle of the HEMs are set to bounce and pitch frequencies of the powertrain, respectively. In the PMS shown in Figure 3, Eng and Eng-front mounts are used for controlling bounce and pitch vibrations, so the peak frequencies in the loss angle of the two HEMs are set to 9 Hz and 12 Hz, respectively. The dynamic stiffness and loss angle for Eng and Eng-front mounts are given in Figures 6 and 7, respectively.

If the Eng and Eng-front mounts in the PMS are HEMs, and the dynamic stiffness and loss angle are illustrated in Figures 6 and 7, respectively, the PMS is defined as PMS II. If the Eng and Eng-front mounts in PMS II are replaced by rubber mounts corresponding to the rubber spring of the two HEMs, the PMS is defined as PMS I. The Trans and Trans-rear mounts are identical in PMS I and PMS II. The loss angles of a rubber mount are in the range of 2.5 to 12 degrees depending on the Shore hardness of the rubber (Zhang and Shangguan, 2006).

4.3.1. Response to ground excitation

Dynamic amplitude versus frequency responses of the powertrain C.G. for PMS I and PMS II under a displacement excitation of 1.0 mm amplitude from the ground in the vertical direction are shown in Figures 8 and 9, respectively. It is seen from Figure 8(a) that the displacement amplitude in the Z- direction reaches its maximum at 9.3 Hz (the natural frequency of the powertrain in Z-direction). In PMS II, the Eng mount (an HEM) is used to control the powertrain vibration in the Z- direction, so the maximum displacement of the powertrain C.G. in the Z-direction is greatly reduced as shown in Figure 9(a). Since the dynamic stiffness of an HEM is greater than that of its rubber spring (Shangguan and Lu, 2004), the peak frequency of the displacement in the Z-direction for the powertrain in PMS II shifts to a little higher value compared with the peak frequency in Figure 8(a).

As Table 10 indicates, the vibration of the powertrain

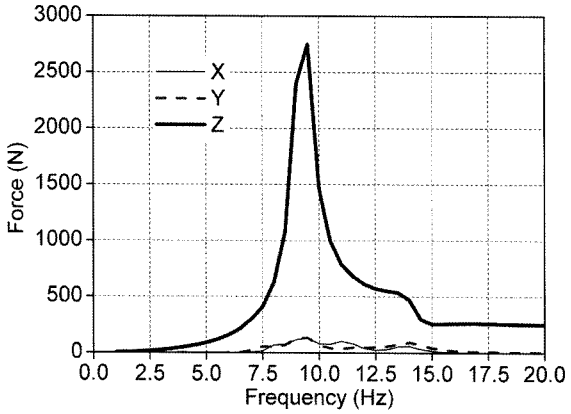

(a) Eng mount

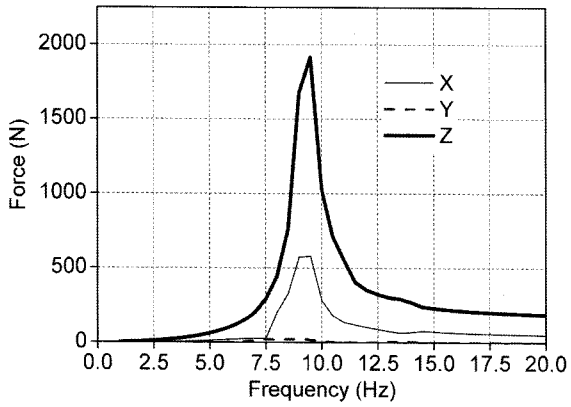

(b) Eng-front mount

Figure 10.The reaction force response of Eng and Eng-front mount in PMS I under ground excitation.

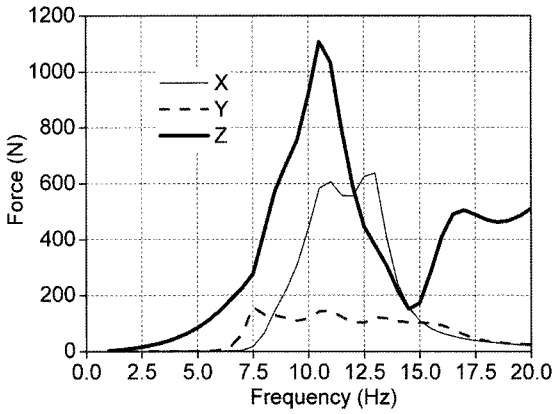

(a) Eng mount

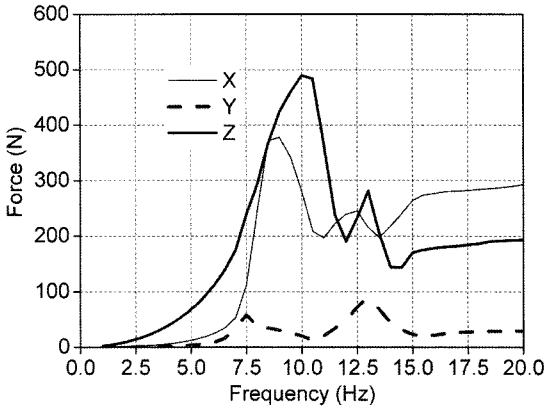

(b) Eng-front mount

Figure 11. The reaction force response of Eng and Eng-front mount in PMS II under ground excitation.

in the pitch direction is coupled with the *X*- and roll directions, so the amplitude of the pitch response of the powertrain in PMS I reaches its maximum value at 8 Hz, 11.6 Hz and 14 Hz, respectively, which corresponds to the natural frequencies of the powertrain in the *X*-, pitch and roll directions. For the same reason, the amplitude of the powertrain response in the roll and yaw directions reaches its maximum value at 14 Hz. It is also seen from Figure 8(b) that the amplitude of the roll, pitch and yaw response of the powertrain reaches its maximum value at 9.3 Hz (a natural frequency of the powertrain in *Z*-direction), since the powertrain vibrates mostly in the Z-direction under ground excitation.

The amplitude versus frequency responses (A-F responses, for short) of the powertrain in the roll, pitch and yaw directions for PMS II is shown in Figure 9(b). It is seen that only one peak value occurs for the pitch and yaw responses, and the peak frequencies correspond to the natural frequencies in the pitch and yaw directions, respectively. This calculated result demonstrates that the coupling of the powertrain vibration is decreased with the use of HEMs in PMS II.

Since the excitation to the powertrain is in the vertical direction, the powertrain angle displacements in the roll, pitch and yaw directions for PMS I and PMS II are small overall as Figures 8(b) and 9(b) indicate. Since the dynamic stiffness of an HEM is greater than that of its rubber spring, the angle displacement responses of the powertrain in PMS II increase a little.

The A-F responses of the reaction forces at Eng and Eng-front mount in PMS I and PMS II are illustrated in Figures 10 and 11, respectively. It is seen that the peak value and the amplitude of the reaction forces overall at the mounts in PMS II are reduced greatly with the use of HEMs. This increases the fatigue life of brackets and decreases the booming noise inside the cab induced by cab vibration.

4.3.2. Response to torque impulse excitation

When the output torque of the powertrain changes, a torque impulse load is applied to the powertrain in the pitch direction of the GCS for the PMS shown in Figure

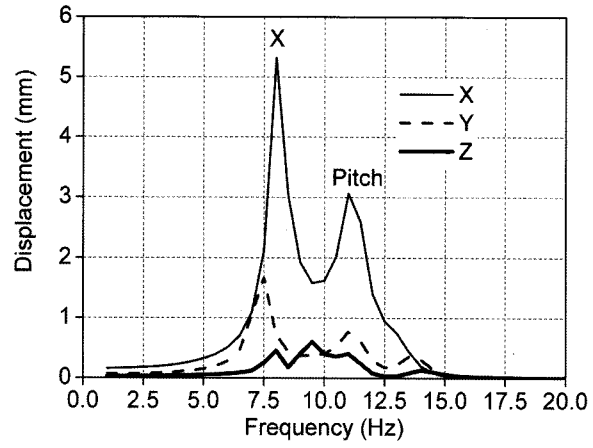

(a) Translation displacement

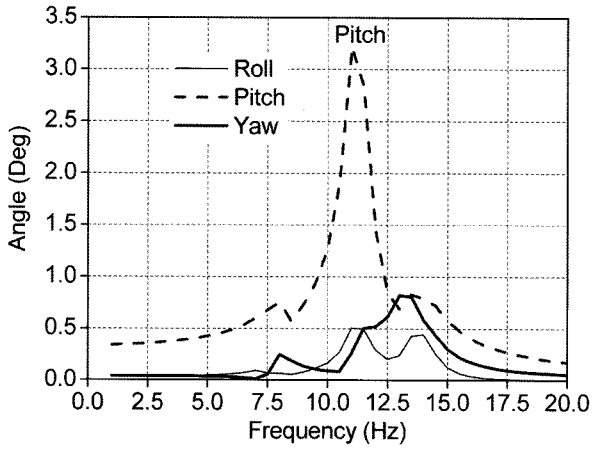

(b) Angle

Figure 12. The amplitude versus frequency response of the powertrain *C.G.* for PMS I under torque excitation.

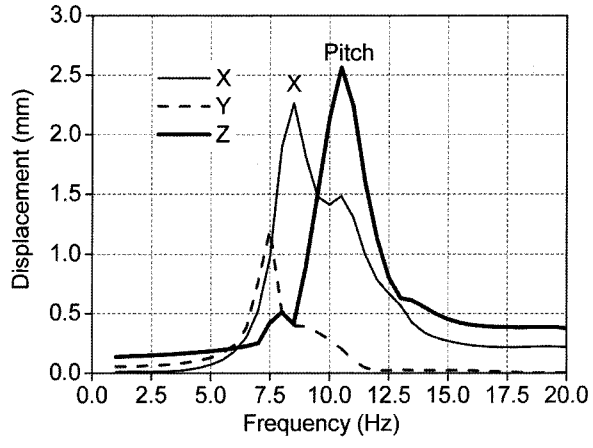

(a) Translation displacement

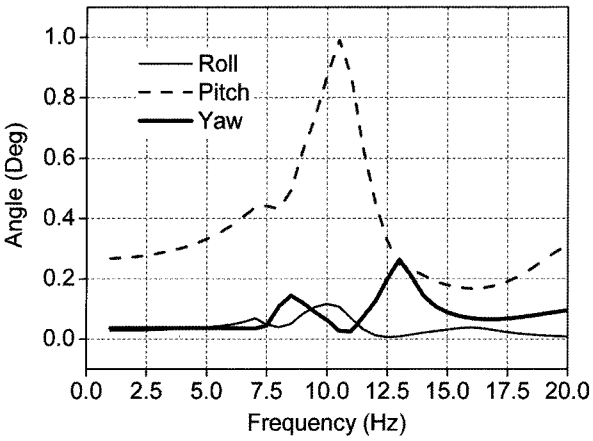

(b) Angle

Figure 13. The amplitude versus frequency response of the powertrain C.G. for PMS II under the torque excitation.

3. Assuming the amplitude of the torque impulse is 200 N.m (The maximum output torque of the engine), the A-F responses of displacements of the powertrain C.G. for PMS I and PMS II are shown in Figures 12 and 13, respectively. It is seen from Figures 12(b) and 13(b) that under torque excitation in the pitch direction, the pitch response of the powertrain reaches its maximum at the natural frequency of the powertrain in the pitch direction (11.6 Hz). The Eng-front mount in PMS II is an HEM, and is used mainly to control the pitch vibration of the powertrain when the output torque of the powertrain changes. So the peak value in the pitch response in PMS IIis reduced greatly than that in PMS I, which demonstrates that the resonance peak of the powertrain in the pitch direction under the torque impulse excitation can be reduced effectively using an HEM designed on the basis of the proposed methods.

As Figure 12(a) indicates, the vibration of the powertrain in the pitch and *X*- directions is coupled, so the response in the *X*- direction reaches maximum values at 8 Hz and 11.6 Hz, which corresponds to the natural frequencies of the powertrain in the *X*- and pitch directions, respectively. It is shown in Figure 13(a) that the displacement responses of the powertrain in PMS II in the *X*-, *Y*- and *Z*- directions reach maximum values at 8 Hz, 7.5 Hz and 11.6 Hz, respectively, which demonstrates that the powertrain vibrates not only in the pitch direction but also in three translation directions.

The A-F responses ofthe reaction forces at Eng and Eng-front mounts in PMS I and PMS II are given in Figures 14 and 15, respectively. It is seen from Figure 14 that the reaction forces at the Eng mount in the *X*-direction and at the Eng-front mount in the *Z*- direction reach its maximum value at 11.6 Hz (a natural frequency of powertrain in pitch direction) under torque excitation.

Since vibrations of the powertrain in the *X*-and pitch directions are coupled, it is seen from Figure 14(b) that

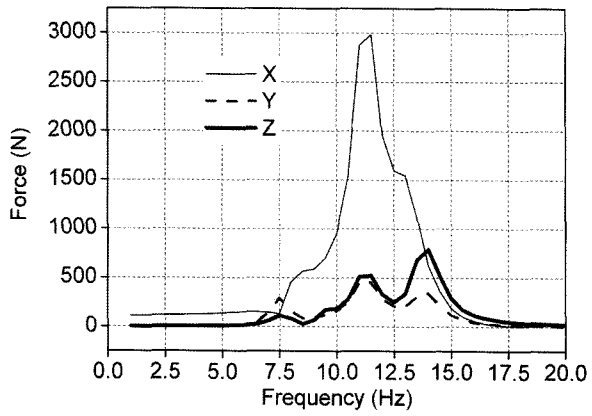

(a) Eng mount

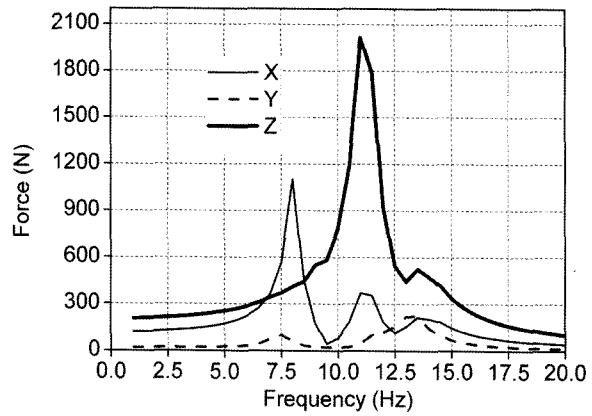

(b) Eng-front mount

Figure 14. The reaction force response of Eng and Eng-front mount in PMS I under torque excitation.

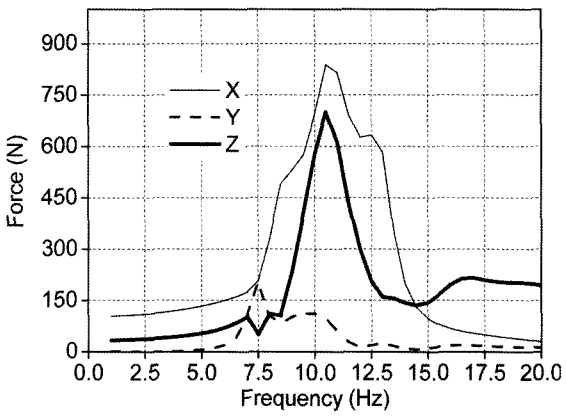

(a) Eng mount

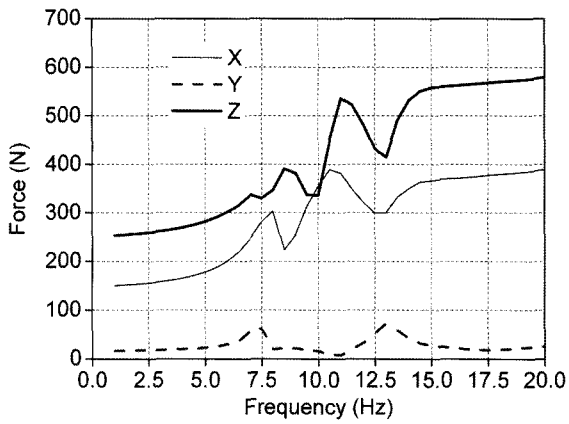

(b) Eng-front mount

Figure 15. The reaction force response of Eng and Eng-front mount in PMS II under torque excitation.

the reaction force at the Eng-front mount in the *X*-direction reaches its maximum at 8 Hz (a natural frequency of powertrain in *X*- direction) under torque excitation. As Figure 15 indicates, reaction forces at the Eng and Eng-front mounts of PMS II in the *Z*- and *X*-directions reach maximum values at 11.6 Hz, but the peak value and the amplitude overall is reduced largely with the use of HEMs in PMS II.

5. CONCLUSIONS

A method for the dynamic analysis and design calculation of a PMS using HEMs is developed using Newton's second law with the aim of controlling powertrain motion and low-frequency vibration in pitch and bounce modes in GCS. Furthermore, the method is validated by analyzing responses of a generic PMS with four rubber mounts or two rubber mounts and two HEMs. In modeling a PMS, the powertrain is modeled as a rigid body connected to a rigid ground by rubber mounts and/or HEMs. The mount in PMS is simplified as a three-dimensional spring and damping elements in each direction of its LCS. The F-D relation of each mount in its LCS is usually nonlinear and is simplified as piecewise linear at five ranges in this paper. Equations for estimating displacements of the powertrain C.G. and a mount in its LCS, and reaction forces at each mount under static or quasi-static loads are developed, and an iterative calculation method is presented. The static stiffness and coordinates of the tuning points in the line of F-D relation for each mount in its LCS are determined by criteria of powertrain motion control. Calculated displacement results of the powertrain C.G. under static or quasi-static loads show that the powertrain motion can meet the displacement limits by properly selecting the stiffness and coordinates of the tuning points of each mount in its LCS with the aid of the calculation methods proposed in this paper.

The equation for analyzing dynamic displacement responses of the powertrain C.G. under ground and engine shake excitations are derived using Newton's second law and the formulae for calculating dynamic reaction forces at each mount are presented. Computer

simulation results of dynamic responses of a powertrain demonstrates that resonance peaks of the powertrain displacements and reaction forces at mounts can be effectively reduced with the HEMs designed on the basis of the proposed methods.

This paper contributes to literature on powertrain dynamics by proposing a method for estimating displacements of powertrain C.G. when the F-Drelation of each mount in its LCS is piecewise linear, and also proposes a calculation and analysis method for reducing resonance peaks of the powertrain in a PMS using HEMs.

ACKNOWLEDGEMENTS–The authors gratefully acknowledge the financial support of the Natural Science Foundation of China (No. 50575073), the science fund of State Key Laboratory of Automotive Safety and Energy (No. KF2006-06).

REFERENCES

Bernard, J. E. and Starkey, J. M. (1983). Engine mount optimization. *SAE Paper No.* 830257.

Brach, R. M. (1997). Automotive powerplant isolation strategies. *SAE Paper No.* 971942.

Cho, S. (2000). Configuration and sizing optimization of powertrain mounting systems. *Int. J. Vehicle Design* **24**, **1**, 34–37.

Demic, M. (1990). A contribution to the optimization of the position and the characteristics of a passenger car powertrain mounts. *Int. J. Vehicle Design* **11**, **1**, 87–99.

Geck, P. E. and Patton, R. D. (1984). Front wheel drive engine mount optimization. *SAE Paper No.* 840736.

Haug, E. J. (1989). *Computer Aided Kinematics and Dynamics of Mechanical Systems, I: Basic Methods.* Allyn and Bacon. Needham Heights. MA.

Ishihama, M., Seto, K., Nagamatsu, A. and Kazuhiro D. (1995). Control of engine roll and bounce vibration using hydraulic mounts. *JSME Int. J. (Series C)* **38**, **1**, 29–35.

Johson, S. R. and Subhedar, J. W. (1979). Computer optimization of engine mounting systems. *SAE Paper No.* 790974.

Qatu, M., Sirafi, M. and Johns, F. (2002). Robustness of powertrain mount system for noise, vibration and harshness at idle. *Proc. Instn. Mech. Engrs, Part D, J. Automobile Engineering,* **216**, 805–810.

Shangguan, W.-B. and Lu, Z.-H. (2004). Experimental study and simulation of a hydraulic engine mount with fully coupled fluid structure interaction finite element analysis model. *Computers & Structures* **82**, **22**, 1751–1771.

Sirafi, M. and Qatu, M. (2003). Accurate modeling for powertrain and subframe models. *SAE Paper No.* 2003-01-1469.

Snyman, J. A., Heuns, P. S. and Vermeulen, P. J. (1995). Vibration isolation of a mounted engine through optimization. *Mechanism and Machine Theory* **30**, **1**, 109–118.

Suh, M. W., Shim, M. B., Kim, M. S. and Hong, S. K. (2003). Multidisciplinary design optimization of engine mounts with consideration of the driveline. *Proc. Instn. Mech. Engrs, Part D, J. Automobile Engineering,* **217**, 107–113.

Swanson, D. A., Wu, H. T. and Ashrafiuon, H. (1993). Optimization of aircraft engine suspension systems. *J. Aircraft* **30**, **6**, 979–984.

Tao, J. S., Liu, G. R. and Lam, K. Y. (2000). Design optimization of marine engine mount system. *J. Sound and Vibration* **235**, **3**, 477–494.

Vietor, T., Deges, R., and Hampl, N. (1997). Robust design of elastic mounting systems. *SAE Paper No.* 971933.

Yu, Y. H., Naganathan, N. G. and Dukkipati, R. V. (2001). A literature review of automotive engine mount systems. *Mechanism and Machine Theory* **36**, **1**, 123–142.

Zavala, P. A. G., Pinto, M. G., Pavanello, R. and Vaqueiro, J. (2000). Experimental and computational simulation approaches for engine mounting development and certification. *SAE Paper No.* 2000-01-3239.

Zhang, Y.-Q. and Shangguan, W.-B. (2006). A novel approach for low-frequency performance design of hydraulic engine mounts. *Computers & Structures* **84**, **7/8**, 572–584.